Acta Poloniae Pharmaceutica – Drug Research, Vol. 76 No. 3 pp. 453–468, 2019
DOI: 10.32383/appdr/102651
ISSN 0001-6837
Polish Pharmaceutical Society

DRUG SYNTHESIS

DESIGN, SYNTHESIS AND BIOLOGICAL ESTIMATION OF INNOVATIVE PYRAZOLES AS ANTICANCER AGENTS TARGETING CDK2

IBRAHIM ALI M. RADINI[1], DIAA A. IBRAHIM[1,2]* and RIZK E. KHIDRE[1,3]

[1]Chemistry Department, Faculty of Science, Jazan University, Jazan, Saudi Arabia
[2]National Organization for Drug Control & Research, P.O. Box: 29, Giza 12311, Egypt
[3]Chemical Industries Division, National Research Center, Dokki, 12622, Giza, Egypt

Abstract: CDK2, which exhibits an indispensable role as an organizer of cell growth, is the powerfully studied protein Kinases objective of anticancer suppressors. The present study was dedicated to design (pharmacophore, docking, and binding energy) and to prepare an inspired derivatives of pyrazole and pyrazolo[1,5-d]pyrimidine as promising anticancer agents, which can act by targeting CDK2. The promising compounds were selected according to their fit-value and binding energy scores. The anticancer activity against MCF-7 was tested for the prepared compounds and compounds **2**, **3b**, and **7b** showed expressive activity with IC_{50} 1.75, 0.89 and 1.32 μM respectively. The CDK2 evaluation was carried out to estimate the efficiency of the prepared compounds as promising inhibitors. The results revealed that compound **3b** with effective inhibitory activity against tumor growth and with its potent inhibition against the CDK2 enzyme with percent inhibition 86 would be a prospective anticancer agent. The prepared compounds with high biological activity could be used as lead inhibitors for the CDK2 kinase domain.

Keywords: pyrazoles, pyrazolo[1,5-d]pyrimidines, CDK2 inhibitors, pharmacophore, docking study, binding energy, anti-proliferative activity

Cancer is a characteristic disease, which displays an indefinite growth, invasion, and metastasis. Approximately most cancers are established by an irregularity in the hereditary material of the deformed cells. These irregularities could be completed by the effects of carcinogens, similar to tobacco smoke, radiation, chemicals, or contagious factors. Further cancer- enhancing genetic deviations could be randomly developed within faults in DNA replication, or are congenital, and thus existing in the cells from date of birth. The heritability of cancers is frequently exaggerated by many interaction steps between carcinogens and the host's genome. New points of the genetics of malignancy pathogenesis, like DNA methylation, and micro-RNAs are known as crucial factors.

Protein kinases are a category of enzymes that are elaborated in a reversible chemical reaction, in which a phosphate group of ATP, or, more seldom GTP, is moved to a protein target (1, 2). This procedure is reversible and is preserved by the existence of other enzymes, called phosphatases, which catalyze the reverse reaction (3) and the imbalance between these enzymes could increase the chance of diseases incidence. More than 400 human diseases, such as diabetes, rheumatoid arthritis, many malignancies, and viral diseases, are attributable to irregular planes of phosphorylation by kinases (1, 4).

Cyclin-dependent Kinases (CDKs) are a class of preserved serine/threonine kinases. Until now, thirteen CDKs have been recognized in mankind (5). CDKs' organization is a result of the combination with a protein, a cyclin (25 types are known). It is distinguished that the expression of CDKs last constant, while cyclin levels change through the cell cycle. Irregular expression of cyclins takes a direct effect on cell deregulation that may drive tumor progress (4) that make it a treasured target for treating cancer. CDKs can be divided into two sets, the first ones facilitate cell progression (CDK1-4 and CDK6), and the second ones organize transcription (CDK7-CDK9 and CDK11-CDK13).

On the other hand pyrazole nucleus characterizes a prevalent core in many pharmaceutical com-

* Corresponding author: e-mail: diaarnm@gmail.com

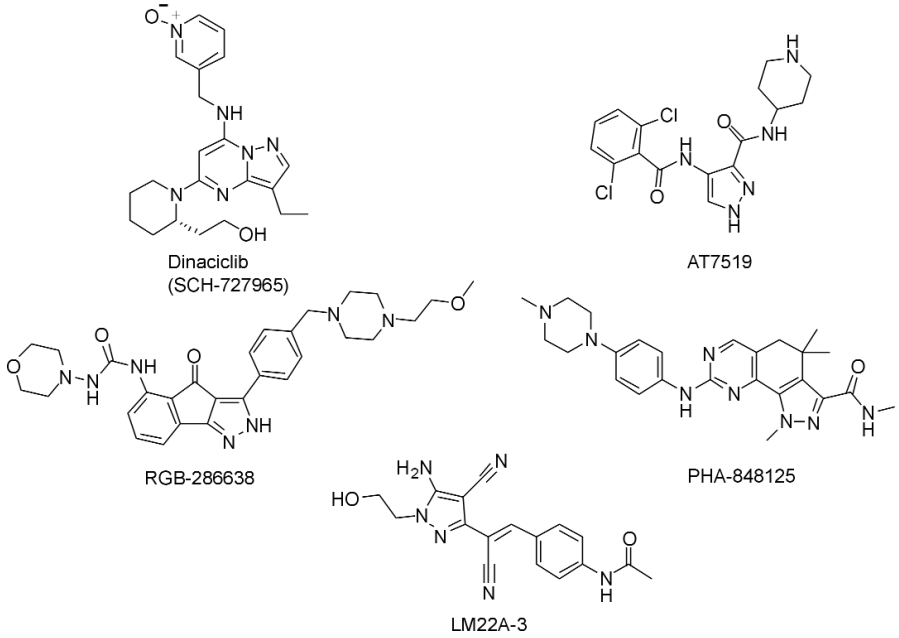

Figure 1.Some pyrazole derivatives under clinical evaluation as Cyclin-dependent kinase inhibitors

pounds and suggesting a varied range of pharmacological activities such as anti-inflammatory (6, 7), antibacterial, antifungal (8, 9), hypoglycemic (10, 11), anti-hyperlipidemic (12), cyclooxygenase-2 inhibitors (13), p38 MAP kinase (14), CDK2/Cyclin A inhibitors (15, 16), and antiangiogenic (17). They similarly signify an elegant choice as a starting substance for producing pharmaceutical compounds that own different activities and display good safety profiles (18).

One of the vital fused pyrazoles is pyrazolopyrimidines which have a diversity of biological activities (19). Plentiful pyrazoles have also been inspected for their antiproliferative actions *in-vitro* and antitumor activity *in-vivo* leading to encouraging lead compounds (20) (Fig. 1).

Regarding the exploring of small produced compounds with anticancer activities, (21-26) this study revealed a modified approach to access the pyrazole and fused pyrazole derivatives framework. Hither, we depict the design, the synthetic strategy and the biological estimation of the synthesized compounds.

EXPERIMENTAL SECTION

General information

All chemicals utilized in this study were bought from SD-fine (India) and Sigma–Aldrich (USA) and were applied without any further purification. Separation and purification of the new compounds were achieved via column chromatography, whenever possible via silica gel 60 (200–300 mesh). The reactions progress was checked by TLC and visualized by UV light (254 nm). Melting points (uncorrected) were measured by an XT4 M. P. apparatus. Mass spectra were listed on a Varian MAT 112 spectrometer AL-Azhar University. Analytical data (IR) were achieved at Jazan University and National Research Center. ^{1}H NMR spectra were recorded on a Variant spectrometer 500 MHz, at the Micro-Analytical Data Center of Mansoura University and at the National Research Center with TMS as internal standards. Chemical shifts were stated in ppm (δ). Elemental analyses were done on a CHN-Rapid instrument in the Micro-Analytical Data Center at Al-Azhar University and the main laboratories of the chemical war.

Synthesis

3-(Cyanomethyl)-5-(1,3-dioxoisoindolin-2-yl)-1H-pyrazole-4-carbonitrile 2

Phthalic anhydride (1.48 g, 10 mM) and 5-amino-3-(cyanomethyl)-1H-pyrazole-4-carbonitrile **1** (1.47 g, 10 mM), were refluxed in glacial acetic acid (50 mL) for 6 h then the reaction mixture was filtered off while hot and the solvent was evaporated. The solid separated was triturated with water, fil-

tered and recrystallized from methanol. Yield 91%; off white solid; M. p. 165-167°C; FTIR (KBr, ν/cm^{-1}): 3250 (NH), 2239, 2222 (2CN), 1797, 1735 (2C=O), 1610 (aromatic C=C); ^{1}H NMR (500 MHz, DMSO-d_6) δ 11.81 (s, 1H, NH), 7.97 (dd, *J* = 7.5 Hz, 2H), 7.88 (t, *J* = 7.5 Hz, 2H), 3.93 (s, 2H, CH_2); ^{13}C NMR (125 MHz, DMSO-d_6) δ 167.19, 136.41, 132.27, 130.46, 129.43, 128.98, 128.16, 112.39, 52.49, 15.91; MS (m/z) = 277 (M^+, 100). Analysis: calcd. for $C_{14}H_7N_5O_2$: C, 60.65; H, 2.55; N, 25.26; found: C, 60.49; H, 2.37; N, 24.85.

3-(1-Cyano-2-(substitiutedphenyl) vinyl)-5-(1,3-dioxoisoindolin-2-yl)-1H-pyrazole-4-carbonitrile 3a-c

To a mixture of 3-(cyanomethyl)-5-(1,3-dioxoisoindolin-2-yl)-1H-pyrazole-4-carbonitrile **2** (2.77 g, 10 mM) and the appropriate aldehyde (12 mM) in glacial acetic acid (70 mL) was added freshly fused sodium acetate (4.1 g, 5 mM). The reaction mixture was refluxed for 12 h. The desired product was obtained upon cooling of the reaction mixture, filtration and washing well with water and alcohol.

3-(1-Cyano-2-(4-hydroxyphenyl)vinyl)-5-(1,3-dioxoisoindolin-2-yl)-1H-pyrazole-4-carbonitrile (3a).

Yield 79%; yellow solid; M.p. 186-188°C; FTIR (KBr, ν/cm^{-1}): 3309 (OH), 3246 (NH), 2960 (C-H), 2227 (CN), 1737, 1708 (2C=O), 1612 (aromatic C=C); ^{1}H NMR (500 MHz, DMSO-d_6) δ 12.50 (s, 1H, NH), 9.34 (s, 1H, OH), 7.98 (s, 1H, =CH), 7.97 (dd, *J* = 7.7 Hz, 2H)7.84 (t, *J* = 7.7 Hz, 2H), 7.63 (d, *J* = 7.5 Hz, 2H), 6.78 (d, *J* = 7.5 Hz, 2H); ^{13}C NMR (125 MHz, DMSO-d_6) δ 165.36, 158.79, 154.05, 147.68, 144.95, 134.27, 132.67, 130.83, 124.93, 122.84, 116.74, 116.33, 114.63, 107.18, 79.58; MS (m/z) = 381. Analysis: calcd. for $C_{21}H_{11}N_5O_3$: C, 66.14; H, 2.91; N, 18.36; found: C, 66.42; H, 2.58; N, 18.15.

3-(1-Cyano-2-(3-hydroxyphenyl)vinyl)-5-(1,3-dioxoisoindolin-2-yl)-1H-pyrazole-4-carbonitrile (3b).

Yield 83%; yellow solid; M. p. 166-168°C; FTIR (KBr, ν/cm^{-1}): 3350 (OH), 3170 (NH), 2916 (C-H), 2231 (CN), 1715, 1705 (2C=O), 1595 (aromatic C=C); ^{1}H NMR (500 MHz, DMSO-d_6) δ 9.96 (s, 1H, NH), 9.89 (s, 1H, OH), 8.07 (d, *J* = 6.6 Hz, 2H),7.89 (s, 1H, =CH), 7.84 (t, *J* = 6.6 Hz, 2H), 7.05 (d, *J* = 7.5 Hz, 1H), 6.98 (s, 1H, ArH), 6.97 (t, *J* = 7.5 Hz, 1H), 6.95 (d, *J* = 7.5 Hz, 1H); ^{13}C NMR (125 MHz, DMSO-d_6) δ 165.36, 157.33, 154.05, 147.68, 143.18, 134.27, 133.21, 132.67, 129.81, 126.23, 124.66, 123.30, 117.24, 116.40, 114.63, 107.60, 79.58; MS (m/z) = 381. Analysis: calcd. for $C_{21}H_{11}N_5O_3$: C, 66.14; H, 2.91; N, 18.36; found: C, 65.98; H, 2.78; N, 18.55.

3-(1-Cyano-2-(4-hydroxy-3-methoxyphenyl)vinyl)-5-(1,3-dioxoisoindolin-2-yl)-1H-pyrazole-4-carbonitrile (3c).

Yield 69%; yellowish-white solid; M. p. 158-161°C; FTIR (KBr, ν/cm^{-1}): 3330 (OH), 3213 (NH), 2226 9CN), 2961 (C-H), 1725, 1709 (2C=O), 1610 (aromatic C=C); ^{1}H NMR (500 MHz, DMSO-d_6) δ 9.98 (s, 1H, NH), 8.92 (s, 1H, OH), 7.97 (d, *J* = 6.9 Hz, 2H), 7.89 (s, 1H, =CH), 7.83 (dd, *J* = 5.6, 3.6 Hz, 2H), 7.64 (d, *J* = 7.5 Hz, 1H), 7.17 (s, 1H, ArH), 6.98 (d, *J* = 7.5 Hz, 1H), 3.83 (s, 3H, OCH_3); ^{13}C NMR (125 MHz, DMSO-d_6) δ 165.12, 153.92, 148.87, 148.11, 147.75, 143.40, 134.34, 132.70, 125.25 – 124.85, 116.67, 115.78, 114.29, 113.60,113.04, 107.51, 79.58, 56.13; MS (m/z) = 411. Analysis: calcd. for $C_{22}H_{13}N_5O_4$: C, 64.23; H, 3.19; N, 17.02; found: C, 63.97; H, 3.28; N, 17.15.

4-Amino-3-(1,3-dioxoisoindolin-2-yl)-1H-thieno[3,4-c]pyrazole-6-carbonitrile (4)

Elemental sulfur (10 mM) was added to a solution of 3-(cyanomethyl)-5-(1,3-dioxoisoindolin-2-yl)-1H-pyrazole-4-carbonitrile **2** (2.77 g, 10 mM) in methanol (60 mL), few drops of triethylamine (0.5 mL) was added and the mixture was refluxed for 8 h. and then left to cool. The resulting solid was filtered off, washed with water and recrystallized from methanol. Yield 63%; brown solid; M. p. 125-128°C; FTIR (KBr, ν/cm^{-1}): 3230, 3205 (NH_2), 3113 (NH), 2231 (CN), 1715, 1707 (2C=O), 1610 (aromatic C=C); ^{1}H NMR (500 MHz, DMSO-d_6) δ 11.81 (s, 1H, NH), 7.96 (d, *J* = 5.6 Hz, 2H), 7.69 (dd, *J* = 5.6, 3.6 Hz, 2H), 6.35 (s, 2H, NH_2); ^{13}C NMR (125 MHz, DMSO-d_6) δ 167.19, 136.41, 132.27, 130.46, 129.43, 128.98, 128.16, 116.48, 112.39, 90.49; MS (m/z) = 309. Analysis: calcd. for $C_{14}H_7N_5O_2S$: C, 54.37; H, 2.28; N, 22.64; found: C, 54.61; H, 2.08; N, 22.55.

2-(4,10-Dioxo-4,10-dihydro-1H-pyrazolo[4',3':5,6]pyrimido[2,1-a]isoindol-3-yl)acetonitrile (5)

To a solution of 3-(cyanomethyl)-5-(1,3-dioxoisoindolin-2-yl)-1H-pyrazole-4-carbonitrile **2** (2.77 g, 10 mM) in glacial acetic acid (70 mL) was added dry ammonium acetate (6.9 g, 9 mM). The reaction mixture was refluxed for 24 h. The desired product was obtained upon evaporation of the reaction mixture and washing well with water and alcohol. Yield 55%; yellow solid; M. p. 173-177°C; FTIR (KBr,

ν/cm^{-1}): 3216 (NH), 2227 (CN), 2961 (C-H), 1704, 1690 (2C=O), 1612 (aromatic C=C); ^{1}H NMR (500 MHz, DMSO-d_6) δ 12.97 (s, 1H, NH), 8.34 (d, *J* = 7.6 Hz, 1H), 8.02 (d, *J* = 7.6 Hz, 1H), 7.81 (t, *J* = 8.2 Hz, 1H), 7.39 (t, *J* = 8.2 Hz, 1H), 4.68 (s, 2H, CH_2); ^{13}C NMR (125 MHz, DMSO-d_6) δ 161.69, 160.73, 149.28, 140.80, 138.00, 135.12, 131.11, 130.46, 128.55, 125.54, 124.27, 116.87, 113.66, 19.28; MS (m/z) = 277. Analysis: calcd. for $C_{14}H_7N_5O_2$: C, 60.65; H, 2.55; N, 25.26; found: C, 60.81; H, 2.38; N, 24.96.

5-(1,3-Dioxoisoindolin-2-yl)-3-(2-oxo-2H-chromen-3-yl)-1H-pyrazole-4-carbonitrile derivatives (6a,b)

To a mixture of 3-(cyanomethyl)-5-(1,3-dioxoisoindolin-2-yl)-1H-pyrazole-4-carbonitrile **2** (2.77 g, 10 mM) and salicylaldehyde or 2,4-dihydroxybenzaldehyde (12 mM) in glacial acetic acid (70 mL) was added freshly fused sodium acetate (4.1 g, 5 mM). The reaction mixture was refluxed for 24 h. The desired product was obtained upon cooling of the reaction mixture, filtration and washing well with water and alcohol.

2.2.9.5-(1,3-Dioxoisoindolin-2-yl)-3-(2-oxo-2H-chromen-3-yl)-1H-pyrazole-4-carbonitrile (6a).

Yield 66%; yellow solid; M. p. 205-208^{o}C; FTIR (KBr, ν/cm^{-1}): 3172 (NH), 2231 (CN), 2989 (C-H), 1725, 1715, 1709 (3C=O), 1613 (aromatic C=C); ^{1}H NMR (500 MHz, DMSO-d_6) δ 11.91 (s, 1H, NH), 8.05 (s, 1H, H_4), 7.97 (d, *J* = 7.6 Hz, 1H), 7.76 (dd, *J* = 5.7, 3.8 Hz, 2H), 7.71 (t, *J* = 7.5 Hz, 2H), 7.58 (d, *J* = 7.7 Hz, 1H); ^{13}C NMR (125 MHz, DMSO-d_6) δ 165.36, 163.08, 153.57, 152.05, 145.53, 134.27, 133.58, 132.67, 131.09, 130.78, 128.54, 126.13,125.25, 124.96, 124.19, 120.23, 80.56; MS (m/z) = 382. Analysis: calcd. for $C_{21}H_{10}N_4O_4$: C, 65.97; H, 2.64; N, 14.65; found: C, 65.75; H, 2.44; N, 14.86.

5-(1,3-Dioxoisoindolin-2-yl)-3-(6-hydroxy-2-oxo-2H-chromen-3-yl)-1H-pyrazole-4-carbonitrile (6b).

Yield 72%; orange solid; M. p. 197-199^{o}C; FTIR (KBr, ν/cm^{-1}): 3360 (OH), 3185 (NH), 2228 (CN), 2960 (C-H), 1732, 1720, 1710 (3C=O), 1608 (aromatic C=C); ^{1}H NMR (500 MHz, DMSO-d_6) δ 12.61 (s, 1H, NH), 9.24 (s, 1H, OH), 8.25 (s, 1H, H_4), 7.97 (d, *J* = 7.9 Hz, 2H), 7.84 (t, *J* = 5.7 Hz, 2H), 7.37 (d, *J* = 7.6 Hz, 1H), 7.02 (s, 1H, H_5), 6.94 (d, *J* = 7.6 Hz, 1H); ^{13}C NMR (125 MHz, DMSO-d_6) δ 165.36, 163.10, 153.17 , 152.05, 150.04, 145.53, 134.34, 133.35, 132.67, 124.65,119.43, 118.50, 117.52, 114.41, 113.92, 111.93, 80.52; MS (m/z) = 398. Analysis: calcd. for $C_{21}H_{10}N_4O_5$: C, 63.32; H, 2.53; N, 14.07; found: C, 63.55; H, 2.74; N, 14.06.

2-(4-Imino-2,4-dihydrochromeno[2,3-b]pyrazolo[3,4-d]pyridin-3-yl)isoindoline-1,3-dione derivatives (7a,b)

To a mixture of 3-(cyanomethyl)-5-(1,3-dioxoisoindolin-2-yl)-1H-pyrazole-4-carbonitrile **2** (2.77 g, 10 mM) and salicylaldehyde or 2,4-dihydroxybenzaldehyde (12 mM) in dry methanol (80 mL) was added few drops of piperidine. The reaction mixture was refluxed for 24 h. The desired product was obtained upon cooling and evaporation of the reaction mixture. The residue was triturated with water, filtration and washing well with water and alcohol provide pure products.

2-(4-imino-2,4-dihydrochromeno[2,3-b]pyrazolo[3,4-d]pyridin-3-yl)isoindoline-1,3-dione (7a).

Yield 69%; yellow solid; M. p. 175-176^{o}C; FTIR (KBr, ν/cm^{-1}): 3230, 3175 (2NH), 2969 (C-H), 1721, 1705 (2C=O), 1612 (aromatic C=C); ^{1}H NMR (500 MHz, DMSO-d_6) δ 10.65 (s, 1H, NH), 10.62 (s, 1H, NH), 8.44 (d, *J* = 7.6 Hz, 2H), 7.86 (s, 1H, H_4), 7.62 (dd, *J* = 7.6 Hz, 2H), 7.56 (d, *J* = 7.5 Hz, 1H), 7.30 (t, *J* = 7.5 Hz, 1H), 6.97 (d, *J* = 7.5 Hz, 1H), 6.49 (t, *J* = 7.5 Hz, 1H); ^{13}C NMR (125 MHz, DMSO-d_6) δ 167.01, 159.27 152.17, 146.90, 142.40, 134.13, 132.67, 129.60, 128.04, 126.63, 125.08, 124.15, 122.09, 118.18, 117.40, 103.18, 94.72; MS (m/z) = 381. Analysis: calcd. for $C_{21}H_{11}N_5O_3$: C, 66.14; H, 2.91; N, 18.36; found: C, 66.05; H, 2.64; N, 18.15.

2-(9-Hydroxy-4-imino-2,4-dihydrochromeno[2,3-b]pyrazolo[3,4-d]pyridin-3-yl)isoindoline-1,3-dione (7b).

Yield 69%; brown solid; M. p. 182-184^{o}C; FTIR (KBr, ν/cm-1): 3420 (OH), 3190, 3145 (2NH), 2959 (C-H), 1719, 1703 (2C=O), 1612 (aromatic C=C); ^{1}H NMR (500 MHz, DMSO-d_6) δ 12.60 (s, 1H, NH), 11.00 (s, 1H, NH), 9.19 (s, 1H, OH), 7.97 (d, *J* = 7.4 Hz, 2H), 7.86 (s, 1H, H_4), 7.84 (t, *J* = 7.4 Hz, 2H), 7.43 (d, *J* = 7.5 Hz, 1H), 6.77 (d, *J* = 7.5 Hz, 1H), 6.75 (s, 1H, H_5); ^{13}C NMR (125 MHz, DMSO-d_6) δ 165.91, 159.28, 153.09, 150.20, 146.92, 142.40, 137.62, 134.20, 132.67, 125.15, 122.66, 118.79, 118.01, 116.64, 113.70, 103.57, 94.72; MS (m/z) = 397. Analysis: calcd. for $C_{21}H_{11}N_5O_4$: C, 63.48; H, 2.79; N, 17.63; found: C, 63.17; H, 2.71; N, 17.35.

2-(Cyanomethyl)-5-methyl-6-oxo-6H-chromeno[3,4-e]pyrazolo[1,5-a] pyrimidine-3-carbonitrile derivatives (10a,b)

To a mixture of acetyl acetic ester (1.3 g, 10 mM), salicylaldehyde (1.22 g, 10 mM) or 2,4-dihydroxybenzaldehyde (12 mM) and 5-amino-3-(cyanomethyl)-1H-pyrazole-4-carbonitrite **1** (2.77 g, 10 mM) was added few drops of piperidine. The reaction mixture was stirred for 15 min after which time acetic acid (20 mL) was added and the mixture was refluxed for 14 h. The desired product precipitate upon cooling of the reaction mixture, simple filtration and washing with dilute ethanol provides analytical pure material.

2-(Cyanomethyl)-5-methyl-6-oxo-6H-chromeno [3,4-e]pyrazolo[1,5-a]pyrimidine-3-carbonitrile (10a).

Yield 52%; orange solid; M. p. 164-166^{o}C; FTIR (KBr, ν/cm^{-1}): 2978 (C-H), 2227 (CN), 1725 (C=O), 1637 (C=N), 1589 (aromatic C=C); ^{1}H NMR (500 MHz, DMSO-d_6) δ 8.65 (d, *J* = 7.5 Hz, 1H), 7.93 (t, *J* = 7.5 Hz, 1H), 7.46 (d, *J* = 7.5 Hz, 1H), 7.45 (t, *J* = 7.5 Hz, 1H), 4.13 (s, 2H, CH_2), 2.57 (s, 3H, CH_3); ^{13}C NMR (125 MHz, DMSO-d_6) δ 195.09, 168.96, 158.40, 154.98, 147.05, 134.47, 130.77, 124.93, 124.41, 118.15, 116.16, 115.94, 112.49, 110.13, 80.74, 43.76, 22.22; MS (m/z) = 315. Analysis: calcd. for $C_{17}H_9N_5O_2$: C, 64.76; H, 2.88; N, 22.21; found: C, 64.47; H, 2.63; N, 22.38.

2-(Cyanomethyl)-9-hydroxy-5-methyl-6-oxo-6H-chromeno[3,4-e]pyrazolo[1,5-a] pyrimidine-3-carbonitrile (10b).

Yield 49%; brown solid; M. p. 188-190^{o}C; FTIR (KBr, ν/cm^{-1}): 3345 (OH), 2981 (C-H), 2231 (CN), 1735 (C=O), 1680 (C=N), 1610 (aromatic C=C);^{1}H NMR (500 MHz, DMSO-d_6) δ 10.28 (s, 1H, OH), 7.84 (d, *J* = 7.5 Hz, 1H), 6.85 (s, 1H, H8), 6.82 (d, *J* = 7.5 Hz, 1H), 4.06 (s, 2H, CH_2), 2.57 (s, 3H, CH_3); ^{13}C NMR (125 MHz, DMSO-d_6) δ 185.43, 162.39, 161.55, 156.12, 152.44, 149.97, 137.45, 129.45, 116.95, 114.28, 111.75, 110.54, 108.09, 102.25, 80.74, 44.70, 18.76; MS (m/z) = 331. Analysis: calcd. for $C_{17}H_9N_5O_3$: C, 61.63; H, 2.74; N, 21.14; found: C, 61.39; H, 2.55; N, 22.08.

Ethyl 3-cyano-2-(cyanomethyl)-5-(substituted phenyl)-7-methyl-4,5-dihydropyrazolo[1,5-a] pyrimidine-6-carboxylate (11a-c).

A mixture consisting of 5-amino-3-(cyanomethyl)-1H-pyrazole-4-carbonitrite **2** (2.77 g, 10 mM), appropriate aldehyde (10 mM), ethyl acetoacetate (1.6 mL, 12 mM), methanol (75 mL), and acetic acid (2 mL) was heated under reflux for several hours until completion of the reaction (12-20 h, monitored by TLC). The solvent was removed under reduced pressure; the solid obtained was treated with water (50 mL) and filtered, washed well with water, dried, and crystallized from methanol.

Ethyl 3-cyano-2-(cyanomethyl)-5-(4-hydroxyphenyl)-7-methyl-4,5-dihydropyrazolo[1,5-a] pyrimidine-6-carboxylate (11a).

Yield 52%; orange solid; M. p. 245-246^{o}C; FTIR (KBr, ν/cm^{-1}): 3345 (OH), 3151 (NH), 2916 (C-H), 2231 (CN), 1690 (C=O), 1680 (C=N), 1631 (aromatic C=C);^{1}H NMR (500 MHz, DMSO-d_6) δ 10.88 (s, 1H, NH), 9.47 (s, 1H, OH), 7.18 (d, *J* = 7.5 Hz, 2H), 6.75 (d, *J* = 7.5 Hz, 2H), 6.08 9 s, 1H, H_5), 4.36 (s, 2H, CH_2), 4.07 (q, *J* = 7.9, 4.9 Hz, 2H, CH_2), 2.40 (s, 3H, CH_3), 1.08 (t, *J* = 7.9 Hz, 3H, CH_3); ^{13}C NMR (125 MHz, DMSO-d_6) δ 167.51, 157.92, 155.91, 148.14, 145.67, 135.17, 128.26, 116.86, 116.34, 116.07, 114.36, 107.86, 80.39, 60.10, 54.11, 18.07, 17.82, 17.11, 14.40; MS (m/z) = 363. Analysis: calcd. for $C_{19}H_{17}N_5O_3$: C, 62.80; H, 4.72; N, 19.27; found: C, 62.57; H, 4.45; N, 19.09.

Ethyl 3-cyano-2-(cyanomethyl)-5-(3-hydroxyphenyl)-7-methyl-4,5-dihydro-pyrazolo[1,5-a] pyrimidine-6-carboxylate (11b).

Yield 50%; orange solid; M. p. 235-238^{o}C; FTIR (KBr, ν/cm-1): 3355 (OH), 3162 (NH), 2946 (C-H), 2227 (CN), 1670 (C=O), 1653 (C=N), 1620 (aromatic C=C);^{1}H NMR (500 MHz, DMSO-d_6) δ 10.93 (s, 1H, NH), 9.43 (s, 1H, OH), 7.25 (t, *J* = 6.6 Hz, 1H), 6.64 (d, *J* = 6.6 Hz, 1H), 6.57 (s, 1H, ArH), 6.51 (d, *J* = 6.6 Hz, 1H), 6.09 (s, 1H, H5), 4.09 (s, 2H, CH_2), 3.98 (q, *J* = 8.0, 3.9, 2H), 2.41 (s, 3H, CH_3), 1.17 (t, *J* = 8.0 Hz, 3H, CH_3); ^{13}C NMR (125 MHz, DMSO-d_6) δ 164.81, 157.38, 154.65, 144.95, 144.67, 142.97, 142.06, 130.23, 129.75, 120.27, 117.62, 116.42, 113.73, 73.11, 59.63, 25.98, 17.91, 16.24, 13.92; MS (m/z) = 363. Analysis: calcd. for $C_{19}H_{17}N_5O_3$: C, 62.80; H, 4.72; N, 19.27; found: C, 62.56; H, 4.48; N, 19.09.

Ethyl 3-cyano-2-(cyanomethyl)-5-(4-hydroxy-3-methoxyphenyl)-7-methyl-4,5-dihydro pyrazolo[1,5-a]pyrimidine-6-carboxylate (11c).

Yield 47%; light yellow solid; M. p. 251-253^{o}C; FTIR (KBr, ν/cm-1): 3330 (OH), 3152 (NH), 2962 (C-H), 2229 (CN), 1669 (C=O), 1660 (C=N), 1610 (aromatic C=C); ^{1}H NMR (500 MHz, DMSO-d_6) δ 10.87 (s, 1H, NH), 9.75 (s, 1H, OH), 7.37 (d, *J* = 7.6 Hz, 1H), 6.94 (s, 1H), 6.75 (d, *J* = 7.6 Hz, 1H), 6.53 (s, 1H, H_5), 4.35 (q, *J* = 8.1 Hz, 2H), 4.08 (s, 1H, CH_2), 3.71 (s, 3H, OCH_3), 2.41 (s, 3H, CH_3), 1.08 (t, *J* = 8.0 Hz, 3H, CH_3); ^{13}C NMR (125 MHz, DMSO-d_6) δ 160.45, 154.61, 151.80,

147.87, 145.92, 145.57, 132.88, 120.72, 116.14, 115.63, 114.33, 110.62, 108.36, 80.34, 60.13, 56.14, 54.10, 18.53, 16.73, 14.41; MS (m/z) = 393. Analysis: calcd. for $C_{20}H_{19}N_5O_4$: C, 61.06; H, 4.87; N, 17.80; found: C, 61.26; H, 4.59; N, 17.61.

CDK2/cyclin A2 inhibition assay

The newly synthesized compounds have been investigated as ATP competitive inhibitors against CDK2 (at conc. 10 µM) by BPS Bioscience Inc. Inhibition of CDK2/cyclinA2 was assayed as previously described using Kinase-Glo Plus luminescence kinase assay kit (Promega). It calculates kinase activity by calculating the quantity of ATP residual in the solution succeeding a kinase reaction, which is correlated with the luminescent signal from the assay and is inversely correlated with the amount of kinase activity. The inhibition activity of the test compound was discovered as the measurement of % inhibition of compounds on the enzyme and IC_{50} (µM), which defined as the concentration obligatory for inhibiting the enzyme by 50%.

Cytotoxicity (MTT assay)

Human Breast (MCF-7) cancer cells were propagated in 75 cm^2 cell culture flasks using RPMI-1640 medium (Gibco-USA) supplemented with 10% (v/v) fetal bovine serum (Gibco-USA) and incubated in 5% (v/v) CO_2 incubator at a temperature of 37°C. Confluent cells were detached using 0.25% (w/v) trypsin solution and 0.05% (v/v) ethylenediaminetetraacetic acid (Gibco-USA) for 5 min. Cells were plated at a concentration of 2 x 10^5 cells/mL in 96-well cell culture plates and incubated at a temperature of 37°C for 24, 48 and 72 hours to attain confluence. The medium was poured out and fresh medium containing several concentrations of Doxorubicin was added for cytotoxicity determination using colorimetric MTT reduction assay. Dead cells were washed with phosphate-buffer Elsa-line (PBS), and 50 µl of MTT stock solution (5 mg/mL) was added to each well. After 4 h incubation period, the supernatants were discarded and the formazan precipitates were solubilized by addition of 50 µl per well of dimethyl sulfoxide (DMSO) or 0.4% (v/v) acidified isopropanol. Plates were incubated in darkness for 30 min at 37°C, and absorbance was measured (at 570 nm) using microplate reader (Biotek ELX -800, USA). To estimate the cell viability percentage, we applied the subsequent equation:

$$\text{Cell viability (\%)} = \frac{\text{OD of treated wells}}{\text{OD of control wells}} \times 100$$

The cell viability (%) was plotted against the tested Doxorubicin concentrations. A statistical value between treated and untreated cells was calculated using one-way ANOVA. Differences at P values less than 0.05 were considered significant. The IC_{50} values of test Doxorubicin were calculated by a Masterplex-2010 software program. The statistical analysis was carried out by using Prism software. Inverted microscope (Nikon-Japan) was applied to study and examine the morphological modifications of cells.

Western blot assay

MCF-7 cells were treated with 3 mM of **3b** and incubated for 0, 1, 8, 24 and 48 h. The cells were lysed by 1X RIPA buffer containing protease and phosphatase inhibitors to quantify the protein concentration by BCA protein assay. 20 mg/well was loaded on 8%, 10%, or 12% SDSPAGE and the protein was transferred onto nitrocellulose membrane 0.45 mm for 90 min at 90 V and blocked with 5% BSA after that was propped against Stat3 and its phosphorylated (10% SDSPAGE), CDK2 and its phosphorylated (8% SDSPAGE) overnight at 4°C. The membrane was subjected to the corresponding IR-conjugated secondary antibodies. β-actin was used as a loading control. LiCOR Odyssey imager was utilized to take pictures to the membrane using ImageJ software to analyze the membrane picture.

Molecular modeling

The docking study was made by Discovery Studio 2.5 (Accelrys, USA). The crystal structure of CDK2 enzyme complexes with the native ligand was downloaded from protein data bank website (PDB) entry 2FVD. Clash corrections, hydrogen optimization, and ligand optimization were performed as well as the vital amino acids in the ligand binding site were identified and used as a guide in our docking study. The docking method was evaluated by re-docking the native ligand into the allocated active site of CDK2 and the RMSD value was determined. Interactive docking using C-Docker was accomplished at its default parameters for all the conformers of each compound of the proposed pyrazole derivatives. Each docked compound was given a score (- C-Docker Energy and – C-Docker Interaction Energy), according to its fit in the ligand binding pocket (LBP) and its binding mod. The docked compounds with high docking score were subjected to binding energy step using PBSA method.

RESULTS AND DISCUSSION

Molecular modeling

Through this study, ligand-based drug design was utilized to design the targeted compounds in

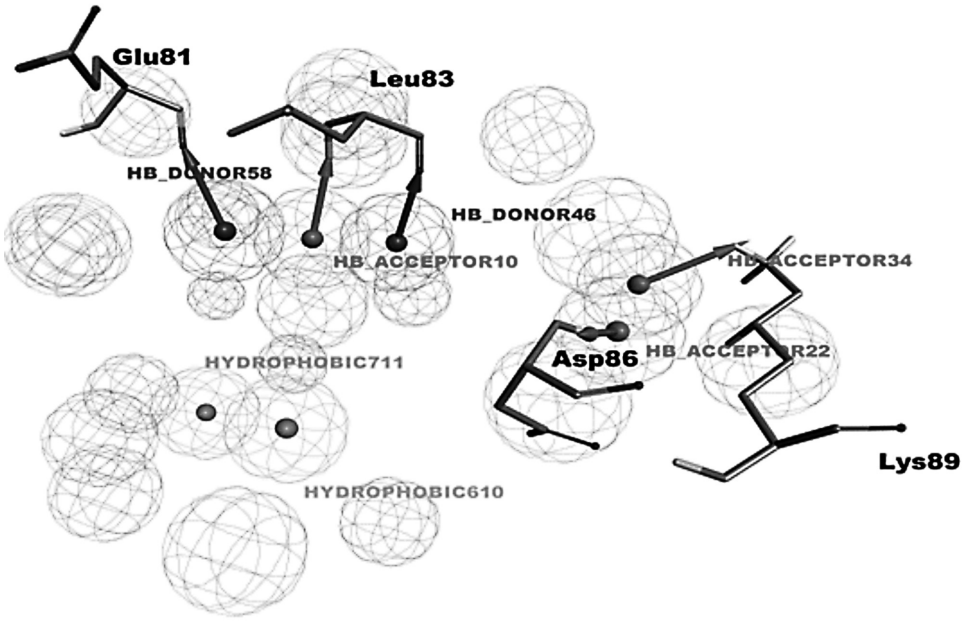

Figure 2. The generated pharmacophore from CDK2 enzyme structure 2fvd (violet for HB donor, green for HB acceptor and cyan for hydrophobes)

Table 1. The recently synthesized compounds with their fit-values, -C-docker interaction energy, binding energy, and total binding energy compared to the native ligand.

Code	Fit values[a]	-C-Docker interaction energy[b]	Binding energy (KCal/mol)[c]	Total binding energy (KCal/mol)[d]
Ligand	5.229	60.683	-42.318	-39.616
2	2.397	30.128	-16.380	-15.216
3a	2.552	39.883	-30.518	-23.517
3b	2.573	42.90	-30.535	-26.052
3c	3.469	44.344	-24.152	-20.824
4	1.913	28.742	-13.578	-13.168
5	2.534	32.829	-24.617	-24.067
6a	2.488	42.317	-26.424	-25.538
6b	2.475	41.788	-33.230	-15.260
7a	1.824	38.351	-30.065	-29.244
7b	2.494	41.613	-32.896	-32.075
10a	1.719	33.044	-26.437	-26.027
10b	1.993	37.095	-23.334	-22.918
11a	2.333	39.686	-31.143	-28.670
11b	2.769	40.886	-31.890	-31.732
11c	2.974	42.557	-40.475	-36.245

[a]Fit value calculated by geometry fitting between the hypothesis and the compound; the higher the value, the better the fit.
[b]The C-DOCKER Interaction energy includes only the interaction energy between the ligand and receptor and is reported in the output SD file of the protocol as the negative of their values (-C-DOCKER ENERGY and -C-DOCKER INTERACTION ENERGY). A negative value of "-C-DOCKER INTERACTION ENERGY" indicates a poor receptor-ligand interaction, so the higher (more positive) value indicates a more favorable binding.
[c]$Energy_{Binding} = Energy_{Complex} - Energy_{Ligand} - Energy_{Receptor}$
[d]$Energy_{Binding} = Energy_{Complex} - Energy_{Ligand} - Energy_{Receptor} - Energy_{Ligand\ conformation}$

three steps, mapping a library of proposed pyrazoles on a specific 3D pharmacophore, docking scores, and binding energy calculations.

Generated pharmacophore and Mapping Library of primary proposed compounds

In this work, we generated pharmacophore model from CDK2 enzyme structure (PDB: 2fvd) for mapping the library of the proposed pyrazoles (150 compounds), (Fig. 2), as an extension to our search hoping to have more potent CDK2 inhibitors. All the inspired pyrazoles were mapped to the generated 3D pharmacophore hypothesis. The strategic compounds with promising fit-values were nominated for the docking and binding energy calculations (Figs 3, 4), (Table 1).

Docking and binding energy studies

The CDK2 coordinates were gained from protein data bank (PDB: 2fvd) and the structure was adjusted by Accelrys Discovery Studio 2.5. The hydrogen atoms and the missing residues were

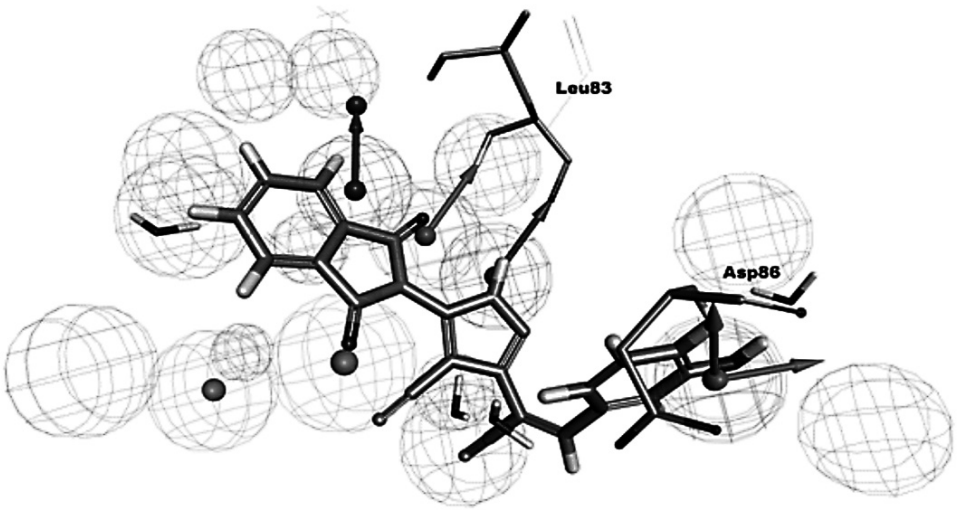

Figure 3. Compound 3b mapped to the generated pharmacophore with fit-value = 2.573 of total 5 features

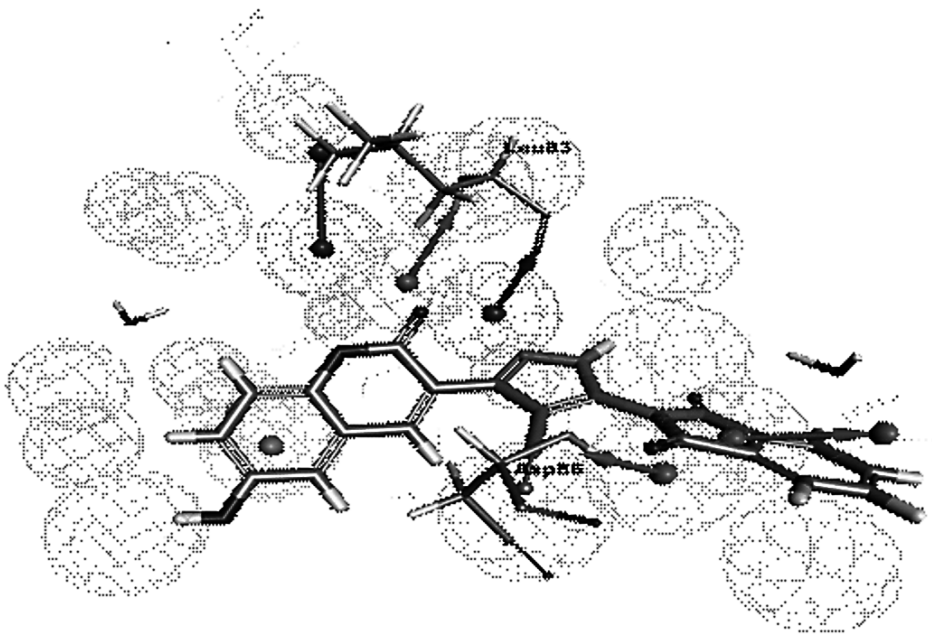

Figure 4. Compound 6b mapped to the generated pharmacophore with fit-value = 2.475 of 5 features

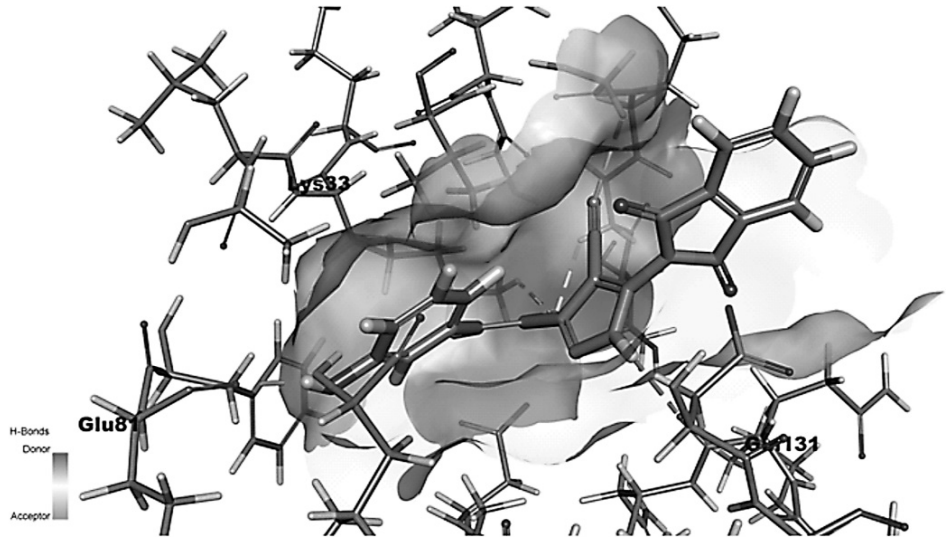

Figure 5. Hydrogen bond interactions of compound 3b in the active site of CDK2 (ATP binding site). It forms 3 HB with Lys33, Gln131 and Glu 81, which is crucial for biological activity

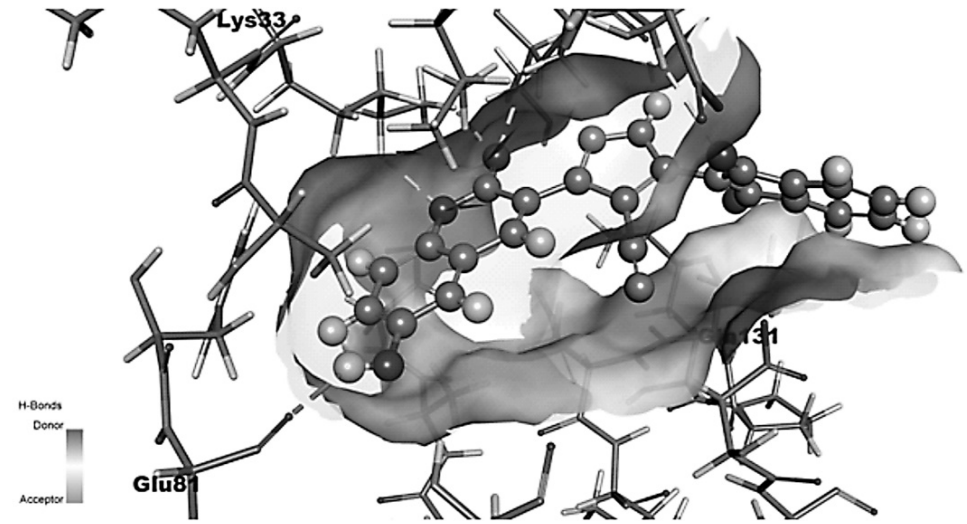

Figure 6. Hydrogen bond interactions of compound 6b in the active site of CDK2 (ATP binding site). It forms 3 HB with Lys33, Gln131 and Glu 81

added as well as the structure was relaxed to correct the protein errors. Finally, the binding site of CDK2 was distinct and all the suggested compounds that met the fit-value standards were nominated for docking and binding energy calculations. the planned compounds were docked by means of the default parameters of C-docker protocol and the hopeful derivatives were elected for preparation (Figs. 5, 6), (Table 1).

Chemistry

The synthesis of substituted pyrazoles has been a topic of formidable attention in organic chemistry (27-29) and our paper presents here a modified process for the preparation of new pyrazole derivatives. The starting material 3-(cyanomethyl)-5-(1,3-dioxo isoindoline-2-yl)-1H-pyrazole-4-carbonitrile **2** was obtained by refluxing compound **1** with phthalic anhydride in acetic acid. The correct struc-

ture of compound **2** was confirmed by IR, which showed the loss of the NH_2 peak at 3350 and 3250 cm^{-1} and exhibited two bands at 1797 and 1735 cm^{-1} because of the two new C=O groups. ^{1}HNMR also showed an increase in the aromatic signals. Reactivity of cyanomethylene towards aldehydes was studied and we managed to obtain the arylidene derivatives **3** in a reasonable yield at refluxing temperature. Also, we react the cyanomethylene group with sulfur according to the conditions of Gewald reaction and the only product was 4-amino-3-(1,3-dioxoisoindolin-2-yl)-1H-thieno[3,4-c]pyrazole-6-carbonitrile **4** in good yield. The assigned structure of compound **4** was confirmed by ^{1}HNMR, which revealed a new signal at 6.8 conformable to the new NH_2 and the CH_2 signal at 4.07 was disappeared. Finally, compound **2** was reacted with ammonium acetate at reflux temperature to give the pyrazolo[3,4-d]pyrimidine derivative **5**, which its structure proved by MS and IR spectrum (Scheme 1).

Coumarins have an extensive scope of pharmaceutical activities, biological functions, and has an excessive reputation in medicine. So, we tried to make a hybrid structure from coumarin and pyrazoles through the reaction of compound **2** with salicylaldehyde derivatives in refluxing acetic acid containing AcONa, and we managed to obtain compounds **6a,b** that proved by ^{1}HNMR, which displayed an increase in the aromatic signals and the vanishing of CH_2 singlet signal at 4.07. Another variation was done by the reaction of compound **2** with salicylaldehyde and 2,4-dihydroxybenzaldehyde in alcohol containing piperidine as a catalyst in a trial to obtain the imino coumarin derivatives, but instead, we obtained 2-(4-imino dihydrochromeno [2,3-b] pyrazolo [3,4-d] pyridine-3-yl) isoindoline-1,3-Dione derivatives **7a, b.** The chemical structures of **7a, b** was established by IR, which showed the disappearance of the two cyano peaks at 2220 and 2225 cm^{-1} and ^{1}HNMR showed the disappearance of CH_2 singlet signal at 4.07 and also, showed a new singlet signal at 10.7 due to the new NH (Scheme 2). MCRs attracted the attention of numerous scientists because they are simpler to perform than multistep syntheses. Also, they had significant progress in the drug invention, and in the identification of pharmaceutical lead compounds through high-throughput screening. So, we prepared compounds **10** and **11** by MCR by reacting compound **1** with different aldehydes and ethyl acetoacetate in refluxing pyridinium acetate as a catalyst (Scheme 3).

Compound **10a, b** was obtained by the reaction of **1** with salicylaldehyde and 2,4-dihydroxy benzaldehyde and its structure was proved by IR that showed a new peak at 1720 cm^{-1} due to C=O of

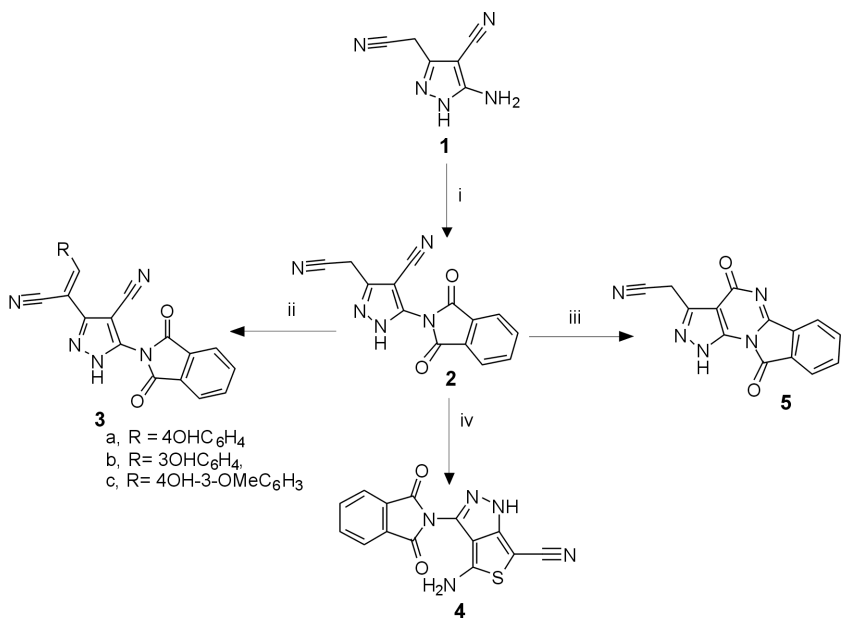

Scheme1. Reagent and condition: (i) Phthalic anhydride, AcOH, reflux; (ii) ArCHO, EtOH, Piperidine, reflux; (iii) NH3, AcOH, reflux; (iv) S, TEA, reflux

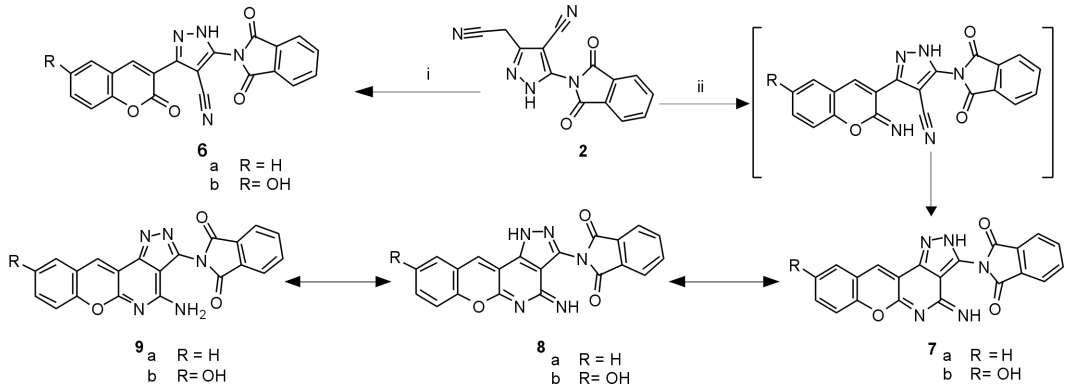

Scheme 2. Reagent and condition: (i) ArCHO, NaOAc, AcOH, reflux; (ii) ArCHO, piperidine, EtOH, reflux

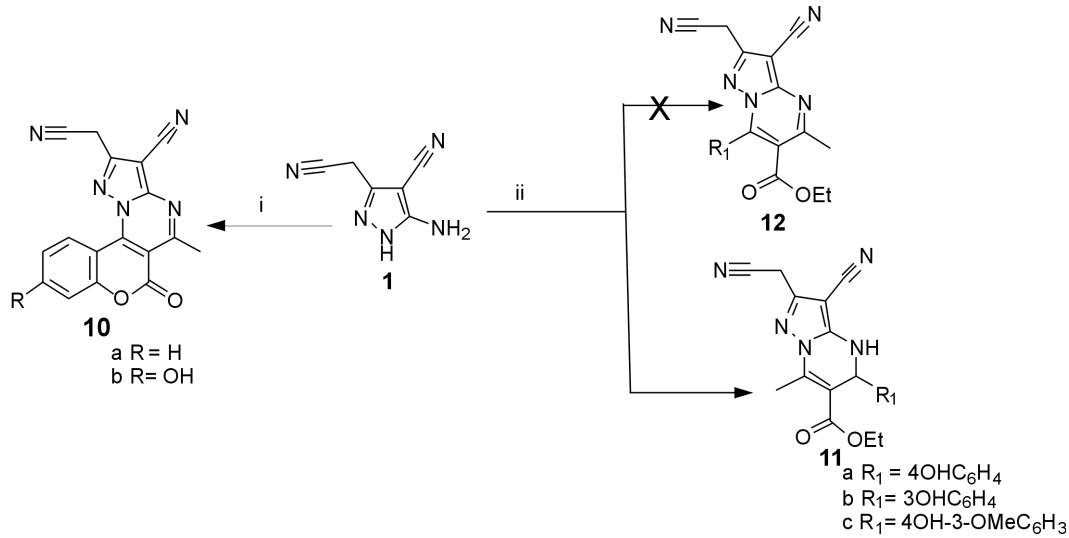

Scheme 3. Reagent and condition: (i) salicylaldehyde derivatives, EAA, piperidine, AcOH, reflux; (ii) ArCHO, EAA, piperidine, AcOH, reflux

coumarin and ^{1}HNMR also, showed new signals in the aromatic region and the disappearance of NH and NH_2 signals at 12.3 and 6.9, respectively. Finally, compound **1** was reacted with aldehydes other than salicylaldehyde derivatives under the same reaction conditions to afford compound **11** or **12** and compound **12** was rolled out because of the absence of NH in the ^{1}HNMR spectrum. The structure of compound **11** was established by ^{1}HNMR, which showed new quartet signal at 3.98 and another triplet signal at 1.18 due to the CH_2 and CH_3 of the new ester group. ^{1}HNMR also showed a new CH_3 signal at 2.4 and revealed the disappearance of NH_2 signal at 6.9.

We suggested that the mechanistic path for the transformation of compound **10** comprised the formation of 3-acetylcoumarins in-situ **12**, which then condensed with aminopyrazolones **1** (Scheme 4). We approved that this method can be directed stepwise by reacting salicylaldehyde with acetyl acetic ester in piperidine as a catalyst at r. t. to afford 3-acetylcoumarin **12** in a quantitative yield. Then compound **12** was furthermore reacted with aminopyrazole **1** in refluxing pyridinium acetate as a catalyst to afford an equivalent yield of polyheterocycles **10a, b** (Scheme 4).

Biology results

Two evaluations of biological tests had been accomplished on the synthesized target compounds: cytotoxicity assay and CDK2/CyclinA assay to estimate the biological profile of the recently synthesized compounds towards CDK2.

In vitro CDK2/cyclin A2 inhibition activity

The well-established compounds were evaluated as CDK2/cyclin A2 and the results showed potent percent inhibition as outlined in (Table 2) and for comparison, Staurosporine was used as positive controls.

By analyzing the percentage inhibition data in (Table 2), we found that seven compounds **2, 3a-c, 4, 5** and **7b** had competitive values more than ATP itself with percentage inhibitory changes values ranging from 60 to 86. Six compounds **6a,b**, **7a**, **10a,b,** and **11b** derivatives showed the moderate

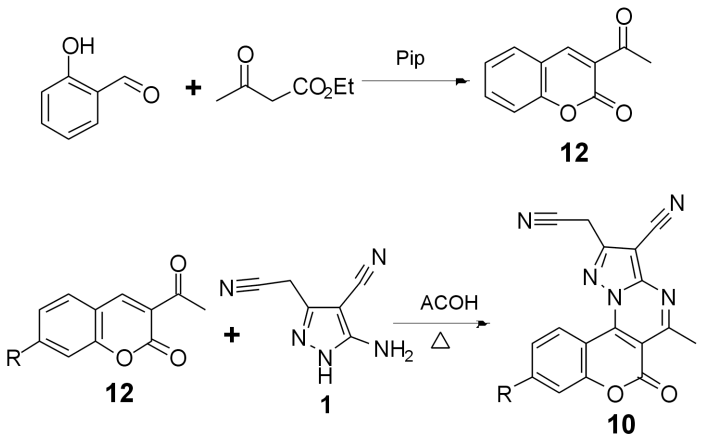

Scheme 4. MCR mechanism[a]

[a] Reagent and condition: 3-acetylcoumarin as an intermediate in the discovered MCR

Table 2. Inhibitory Effects of the newly synthesized compounds on CDK2/cyclin A2 Activity, cytotoxic activity against MCF-7 cell-line and non-cancer breast cell lines.

Compounds	% Inhibition (on CDK2/cyclinA2)[a]	IC_{50} (µM)[b]	
		MCF-7	184B5
2	80	1.75	>100
3a	72	3.73	>100
3b	86	0.89	>100
3c	62	7.39	>100
4	77	2.47	>100
5	60	2.33	>100
6a	48	4.55	>100
6b	31	16.31	>100
7a	35	5.18	>100
7b	69	1.32	>100
10a	37	6.81	>100
10b	44	NT	NT
11a	11	13.19	>100
11b	33	4.46	>100
11c	9	23.91	>100
Staurosporine	100	---	---
Doxorubicin 30, 31	---	1.17	---

[a]50 µL of Kinase-Glo Plus Luminescence kinase assay solution (Promega) was added to each reaction and incubate the plate for 5 minutes at room temperature. The 50 µl reaction mixture contains 40 mM Tris, pH 7.4, 10 mM MgCl2, 0.1 mg/mL BSA, 1 mM DTT, 10 µM ATP, Kinase substrate and the enzyme.

[b]cells were incubated for 72 h with various concentrations of drugs (100 mM stock, then 10 folds serial dilutions). (0, 0.01, 0.1,1, 10, 100 unit) Following 24 and 48 h treatment.

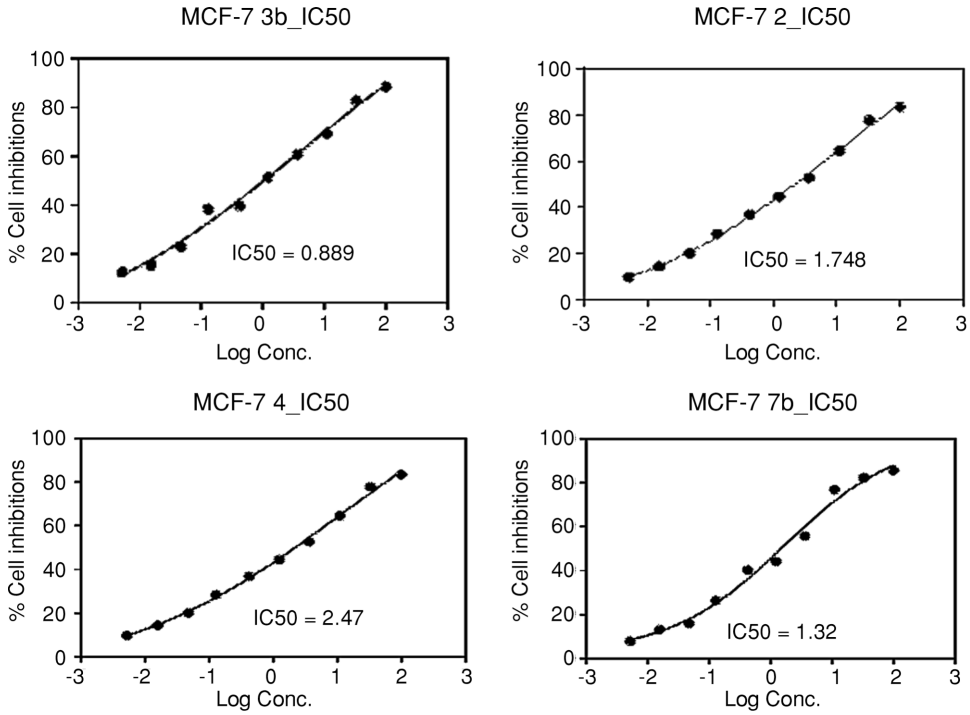

Figure 7. Graph of log compounds 2, 3b, 4 and 7 concentration against % cell inhibitions

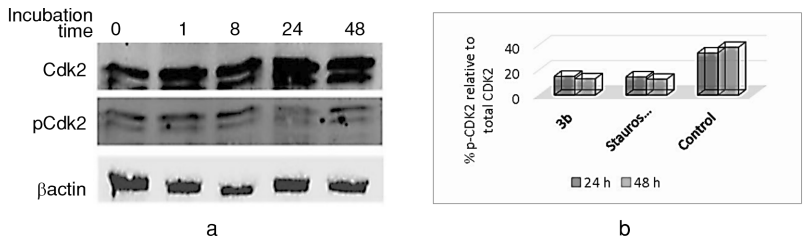

Figure 8. Western blot analysis of MCF-7 cell lysate after treatment with 3 mM of compound 3b for 48 h: a) CDK2 and its phosphorylated form, b) ELISA assay for phosphorylated CDK2 relative to total CDK2 in MCF-7 cell lysate after treatment with 3 mM of compound 3b for 24 and 48 h

competitive inhibitory effect with percent activity changes values ranging from 31 to 48. The remaining compounds (**11a** and **11c**) were found to be inactive with an inhibitory percentage less than 11%.

The biological results showed a good correlation with pharmacophore, docking, and binding energy calculations. The most active compound **2** and **3b** showed the best binding energy calculations due to their good interactions with CDK2 active site (Figs. 3 and 5). Compound 3b, for example, showed good hydrophobic interactions where its phenyl and its phthalimide groups were buried well in the active site. Also, it formed 3 hydrogen bonds with Lys33, Gln131 and Glu 81, which is crucial for biological activity.

Cytotoxicity assay:

The cytotoxicity assay was done to administrate the sensitivity scale and the selectivity of the tested compound against malignant and normal cells. The biological results of the synthesized compounds were measured as IC_{50} against the MCF-7 cancer cell line and 184B5 (Non-malignant mammary epithelial cell) the data were given in (Table 2) (Fig 7). Some of the synthesized compounds displayed higher cytotoxicity against MCF-7 tumor cell

lines but lower cytotoxicity against the 184B5 normal cell line. In the cytotoxicity assay with the MCF-7 cell line, the IC_{50} data declared that compound **3b** demonstrated the highest anticancer activity with an IC_{50} value of 0.89 µM, which is more active than the reference. Since this compound demonstrated the uppermost IC_{50} values so it can be used as a primary hit. Compounds **7b** and **2** presented very high activity versus the cell line reserved for the study with IC_{50} values 1.32 and 1.75 µM respectively. Compounds **4, 5** and **3a** demonstrated good anticancer activity with respect to MCF-7 cancer cell line with IC_{50} values 2.47, 2.33 and 3.73 µM respectively, while the other compounds had a moderate to weak activity. From the formerly detailed investigation of the anticancer activity of our produced compounds against the MCF-7 cell line, we could accomplish that compound **2, 3b** and **7b** exhibited the highest anticancer activity between the examined compounds expressed by their IC_{50} values 1.75, 0.89 and 1.32 µM, respectively related to Doxorubicin IC_{50}= 1.17 µM. The biological profile of these compounds could be improved and could be utilized as lead compounds by further optimization.

The Results of the antitumor screening and CDK2/CyclinA assay revealed that compound **3b** had a high antitumor activity with IC_{50} 0.89 µM and a high CDK2 percent inhibition 86%, which demonstrated that its antitumor action could be owing to the suppression of CDK2 enzyme. Furthermore, compound **3b** could be utilized as a CDK2 lead inhibitor for additional studies. Compound **2, 3a, 4** and **7b** have mild activities as an antitumor mediator, but they have a high CDK2 inhibitory effect with percent inhibition ranges from 69 to 80%.

Western blotting of CDK2 in MCF-7 cells

The promising anti-proliferative activity of **3b** encouraged us to study its effect at the molecular level exploring its potential inhibitory effect to the targets of interest. So, the potential of **3b** to inhibit the phosphorylation of CDK2 at 3 mM within the MCF-7 cell lysate was studied. The phosphorylated CDK2 serves to recruit specific effector molecules to activate several signal transduction pathways that have been implicated pathogenesis of many cancers. The western blot analysis results (Fig. 8a) revealed the potential of 3b to have inhibitory mechanism towards diminishing the phosphorylated levels for CDK2. The obtained data revealed that treatment of MCF-7 cell with 3b for 24 and 48 h diminished CDK2 phosphorylation by about 2 and 3.3 folds

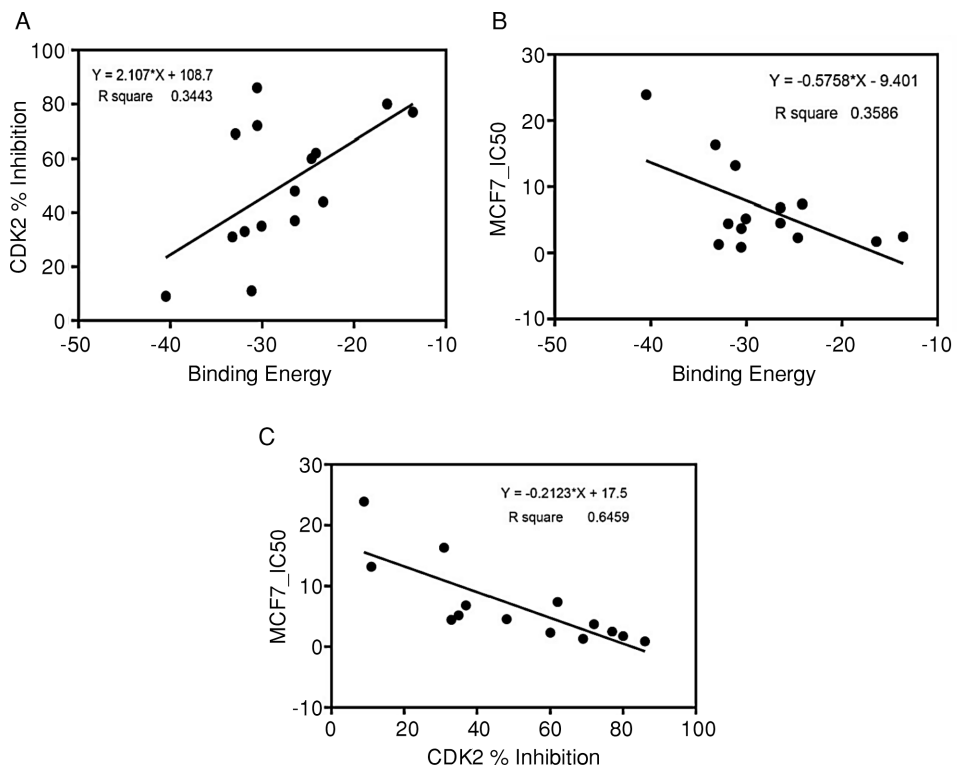

Figure 9. Correlation of binding Energies with CDK2 % inhibition (A) and MCF7-IC50 (B). Correlation of MCF7-IC50 and CDK2 % inhibition (C)

compared to the untreated cell (Control) (Fig. 8b). The ability of **3b** to inhibit the intrinsic kinase activity of CDK2, suggests that it may play a role in suppressing the proliferation of tumors.

To examine the correlation between modeling work and biological results, we carried out the statistical analysis. This analysis indicates that there is a good correlation between CDK2 % inhibition and calculated binding energy for the enzyme with R^2 equal 0.3443 which means that 34.4% of the data are to be fitted to the regression line (Fig. 9A). The P value is 0.0215 typically less than 0.05 which means there is a significant difference between CDK2 % inhibition and calculated binding energy.

On the other hand, the correlation between MCF-7 (IC_{50}) and calculated binding energy showed a slightly higher correlation with R^2 equal 0.3586, which means that 35.9% of the data are to be fitted to the regression line (Fig. 9B). Finally, an excellent correlation is observed between MCF-7 (IC_{50}) and CDK2 % inhibition with R^2 equal 0.646 that means 64.6% of the data are to be fitted to the regression line (Fig. 9C).

The statistical analysis showed that the binding energy is a good tool for drug design and the correlation between MCF7-IC_{50} and CDK2 % inhibition led us to conclude that the antitumor effect of our new compounds was due to the inhibition of CDK2 enzyme with 64.6 % confidence.

CONCLUSIONS

New series of novel pyrazoles were proposed, mapped to CDK2 pharmacophore, docked into the ligand binding site of CDK2 and subjected to binding energy calculation. According to the binding energy calculations the encouraged pyrazoles were chosen for preparation and estimation as inhibitors of CDK2. The obtained pyrazoles showed very good inhibition for antitumor and for CDK2 in µM range. compound **3b** revealed the best activity against MCF-7 cancer cell line with IC_{50} values 0.89 µM, which is more active than the reference. Compound **2, 3a, 4** and **7b** have mild activities as an antitumor mediator, but they have a high CDK2 inhibitory effect with percent inhibition ranges from 69 to 80%, respectively. The remaining compounds showed good to moderate activities. Pharmacophore mapping and binding energy calculation were proved to be a beneficial technique for selecting promising biological candidates. The promising antitumor results of compounds **3b** and **7b** proved that they can be utilized as a significant matrix to design and synthesis of novel candidates with better activities. Further investigation into the other aspects of structure-activity relationship studies of this series of compounds is required to explore the scope and limitation of its anticancer activities.

Acknowledgments

The authors would like to thank the Deanship of Scientific Research, Jazan University, Saudi Arabia for funding this study (project No: JUP7/00089).

Conflicts and interest

The authors declare no conflict of interest

REFERENCES

1. Pinna L.A., Meggio F.: Prog. Cell Cycle Res. 3, 77 (1997).
2. Jans D.A., Hubner S.: Physiol. Rev. 76, 651 (1996).
3. Venter J.C., Adams M.D., Myers E.W., Li P.W., Mural RJ. et al.: Science 291, 1304 (2001).
4. Malumbres M., Barbacid M.: Nat. Rev. Cancer 9, 153 (2009).
5. Etienne S., Nobel Prize in Medicine 2001: Bull. Cancer 88, 937 (2001).
6. Anam A., Abad A., Mohd A. Shams M.: New J. Chem. 41, 16 (2017).
7. György S., János F., Ágnes K., Klára G.: J. Med. Chem. 51, 142 (2008).
8. Akihiko T., Yoshihiro O., Keiko O., Hideo T., Jun-ichi Y.: Bioorganic Med. Chem. Lett. 15, 4299 (2005).
9. Akihiko T., Yoshihiro O., Keiko O., Mika F., Kenji S. et al: Bioorganic Med. Chem. 12, 5515 (2004).
10. Cho N., Kamaura M., Yogo T., Imoto H.: PCT Int. Appl. WO 139340 A1 (2009).
11. Klaus D., Michael M., Frank H.: PCT Int. Appl. WO 022009 A1 (2009).
12. Yu M., Tsuyoshi M., Hiroyuki O., Hiroyuki K.: PCT Int. Appl. WO 038325 A1 (2001).
13. Rida S.M., Saudi M.N.S., Youssef A.M., Halim M.A.: Lett. Org. Chem. 6, 282 (2009).
14. John R., Steffen B., Pier C., Thomas G., Anne G.G. et al.: J. Med. Chem. 45, 2994-3008 (2002).
15. Maria G.B., Clara A., Raffaella A., Dario B., Luca C. et al.: Chem. Med. Chem. 2, 841 (2007).
16. Ashraf H.A., Amal A.E., Ghaneya S.H.: Chem. Pharm. Bull. 51, 838 (2003).

17. Michael R.M.: PCT Int. Appl. WO 065825 A2 (2010)
18. Nasser S.M.I., Eslam M.H.A., Diaa A.I., Rabah A.T.S., Dalal A.A.: FJPS 2, 20 (2016).
19. Alessandro B., Maria A., Chiara M., Cinzia A., Mauro M. et al.: Eur. J. Med. Chem. 46, 5293 (2011).
20. Massa S.M., Yang T., Xie Y., Shi J., Bilgen M. et al: J. Clin. Investig. 120, 1774 (2010).
21. Diaa A.I., Deena S.L., Maysoun Y.Z., Amany W.I., Daniela V. et al.: Bioorg. Med. Chem. 23, 4989 (2015).
22. Diaa A.I., Julie B., Daniel H.L., Sri Kumar V., Kevin R.T. et al.: Bioconjugate Chem. 2403 (2012).
23. Rizk E.K., Ibrahim A.M.R., Diaa A.I.: ARKIVOC (v), 301 (2016).
24. Rizk E.K., Bakr F.A., Ghada E.A.A.: Heterocycles 94, 314 (2017).
25. Rizk E.K., Sameh R.E., Mohamed S.M.: J. Heterocycl. Chem. 54, 2511 (2017).
26. Bakr F.A., Rizk E.K., Hanan A.M., Gamal A.E.: Arab. J. Sci. Eng. 42, 2441 (2017).
27. Alnajjar R.A., Gheath A.H.: Chemica Sinica 5, 97 (2014).
28. Alnajjar R.A., Gheath A.H.: J. Chem. Pharm. Res. 6, 1426 (2014).
29. Soliman A.Y., Bakeer H.M.: Rev. Roum. Chim. 38, 1097 (1993).
30. Nadiah A., Nadeem A., Wan Y.H., Swee K.Y., Noorjahan B.A.: Molecules 18, 10367 (2013).
31. Maliyakkal N., Udupa N., Pai K., Rangarajan A.: Int. J. App. Res Nat. Prod. 6, 1 (2013).

Received: 13.08.2018